International Journal of Innovative Research and Advanced Studies (IJIRAS)
Volume 3 Issue 11, October 2016

ISSN: 2394-4404

Numerical Study On Natural Heat Convection At Various Rayleigh Numbers In A Rectangular Cavity With A Fin On The Cold Wall

K. Gayathri Devi

Research scholar, Department of Mathematics, Sri Krishnadevaraya University, Anantapuramu, A.P., India

R. Siva Prasad

Professor, Department of Mathematics, Sri Krishnadevaraya University, Anantapuramu, A.P., India

Abstract: ***In this paper, we examine the natural heat convection in a rectangular cavity with a fin on the cold wall at various Rayleigh numbers, different lengths and heating locations. Assuming the left and right vertical walls of the cavity are kept at constant temperature and the top and bottom walls of the rectangular cavity are insulated. The Galerkin Finite Elementary Method has been used to convert the Partial Differential Equations into matrix form of equations by dividing the physical domain into smaller segments, which is a pre-requisite for Finite Element Method. Numerical results are presented in terms of stream functions and isotherms for various Rayleigh numbers having with different fin lengths and also with different fin locations. Thus the thin fin is attached to the cold wall increases the cold surface which affects the rate of heat transfer and temperature distribution.***

Keywords: ***Natural heat convective flow; fin on the cold wall; Galerkin Finite Elementary Method; Rayleigh numbers***

I. INTRODUCTION

Free convection fluid flow and heat transfer occurs in many industrial and engineering systems such as solar energy collectors, home ventilation systems, energy storage systems, refrigeration unit, fire prevention etc. In general increasing, controlling, and modification of fluid flow and heat transfer inside the differentially heated cavities is down using a partition or fin attached to the walls of the cavity. Many researchers have investigated natural convection inside cavities with fin on the walls. Frederick [1] studied numerically natural convection in a square enclosure with a thin partition placed at the middle of its cold wall. Decreasing heat transfer of up to 47 percent in comparison with the cavity with no partition was observed in this study. Frederick and Valencia [2] studied heat transfer in a square cavity with a conducting partition located at the middle of its hot wall using numerical simulation. They observed that for a low value of the partition-to-fluid thermal conductivity ratio and for Rayleigh numbers from 10^4 to 10^5 a reduction in heat transfer relative to the case of cavity with no partition occurs. Scozia and Frederick [3] studied numerically heat transfer in a tall cavity with multiple conducting fins on the cold wall. They found that as the inter fin aspect ratio is varied from 20 to 0.25, the flow patterns evolve considerably and the average Nusselt number reaches maximum. Nag et al. [4] investigated the effect of a horizontal thin partition placed on the hot wall of a horizontal square cavity. They observed that for a partition of infinity thermal conductivity the Nusselt number on the cold wall was greater than the case with absence of fin. Lakhal et al. [5] studied that the natural convection in inclined rectangular enclosures with perfectly conducting fins attached to the heated wall.

Bilgen [6] investigated natural convection in cavities with partial partitions positioned on the insulated horizontal walls. He found that the heat transfer was reduced when two partitions were used instead of one, the aspect ratio was made smaller, and the position of partitions was farther away from the hot wall. Shi and Khodadadi [7] reported the results of a numerical study of laminar natural convection in a differentially heated square cavity due to a perfectly conducting thin fin on its hot wall. They found that heat transfer on the cold wall without fin can be promoted for high Rayleigh numbers and with the fins placed closer to the insulated walls. Tasnim and Collins [8] has been studied numerically the heat transfer in a square cavity with a baffle

on the hot wall. Xu and Patterson et al. [10, 11] experimentally studied the thermal flow around a square obstruction on a vertical wall in a differentially heated cavity and also investigated the effect of the thin fin length on the transition of the natural convection flows in a differentially heated cavity. Liu, Lie and Patterson [12] investigated transient natural convection around a thin fin on the side wall of a differentially heated cavity.

Based on these above mentioned articles it was found that to increase the rate of heat transfer inside the differentially heated cavities a highly conductive fin can be attached to the walls of the cavity. In the present study natural convection at various Rayleigh numbers the fluid flow and heat transfer in a differentially heated rectangular cavity with a fin attached to its cold wall is simulated numerically by using Galerkin finite element method. To convert the partial differential equations into a matrix form of equations which are solved iteratively with the help of a computer code. A three nodded triangular elements is used to divide the physical domain into smaller segments.

II. MATHEMATICAL FORMULATION

We consider the natural convective flow of a fluid in a rectangular cavity of width W and height H (H>W) filled with a fluid. The left vertical wall of the cavity is kept at a constant temperature while its right vertical wall is maintained at temperature T_c and T_h ($T_h > T_c$) top and the bottom horizontal walls are kept insulated. A highly conductive thin fin is attached to the cold wall the length and the location of the thin fin on the right wall are shown with *l* and *s* respectively.

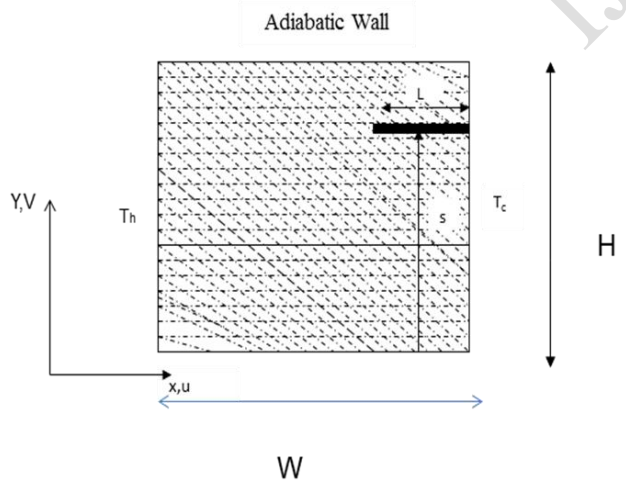

Physical configuration

The dimensionless variables *L = l/W* and *S = s/H* are defined as the length and location of the thin fin respectively. The aspect ratio of the cavity is defined as *Ar = H/L* it is assumed that the fin is highly conductive and is maintained at the same temperature of the wall to which it is attached. The fluid inside the cavity is considered to be incompressible and the two-dimensional flow is assumed to be steady and laminar. The properties of the fluid are assumed to be constant with the exception of the density which varies according to the Boussinesq approximation. Under these above specified geometrical and physical conditions is governed by the momentum and energy can be written as

Continuity equation:

$$\frac{\partial u}{\partial x} + \frac{\partial v}{\partial y} = 0 \qquad (2.1)$$

Heat equation:

$$\frac{\partial v}{\partial t} + u\frac{\partial v}{\partial x} + v\frac{\partial v}{\partial y} = -\frac{1}{\rho}\frac{\partial p}{\partial y} + \vartheta\left(\frac{\partial^2 v}{\partial^2 x} + \frac{\partial^2 v}{\partial^2 y}\right) + g\beta(T - T_c) \qquad (2.2)$$

Energy Equation:

$$u\frac{\partial T}{\partial x} + v\frac{\partial T}{\partial y} = \alpha\left(\frac{\partial^2 T}{\partial x^2} + \frac{\partial^2 T}{\partial y^2}\right) \qquad (2.3)$$

With boundary conditions

u (x , 0) = u(x, L) = u(0 , y) = u(L , y) = 0,

v (x , 0) = v(x, L) = v(0 , y) = v(L , y) = 0,

T (x, 0) = $T_h - T_c$, or T (x, 0) = $(T_h - T_c)\sin\frac{\pi x}{L} + T_c$,

$$\frac{\partial T}{\partial y}(x, L) = 0, \qquad T(0, y) = T(L, y) = T_c.$$

The Continuity equation (2.1) can be satisfied automatically by introducing the stream function 'ψ' as

$$u = \frac{\partial \psi}{\partial y} \quad \text{and} \quad v = -\frac{\partial \psi}{\partial x} \qquad (2.4)$$

where x and y are the distances measured along the horizontal and vertical directions respectively; u and v are the velocity components in the x and y- directions respectively; T denotes the temperature; ϑ - kinematic viscosity; α _ thermal diffusivity; K is the medium permeability; P is the pressure; ρ is the density; T_h and T_c are the temperatures at hot vertical wall and cold vertical walls respectively; L is the length of the conductive thin fin.

Using the following change of variables,

$$\bar{\psi} = \frac{\psi}{\nu}, \qquad U = \frac{uL}{\alpha}, \qquad V = \frac{vL}{\alpha}, \qquad X = \frac{x}{L}, \qquad Y = \frac{y}{L}, \qquad \theta = \frac{T - T_c}{T_h - T_c}.$$

The governing equations (2.1), (2.2) and (2.3) reduced to non-dimensional form and introducing stream function (2.4) we have,

$$\frac{\partial U}{\partial X} + \frac{\partial V}{\partial Y} = 0 \qquad (2.5)$$

$$\left[\frac{\partial \bar{\psi}}{\partial Y}\frac{\partial^2 \bar{\psi}}{\partial X \partial Y} - \frac{\partial \bar{\psi}}{\partial X}\frac{\partial^2 \bar{\psi}}{\partial Y^2}\right] = \Pr\left[\frac{\partial^2 \bar{\psi}}{\partial X^2} + \frac{\partial^2 \bar{\psi}}{\partial Y^2}\right] + \Pr\frac{\partial \bar{\psi}}{\partial Y} - Ra\Pr\theta \qquad (2.6)$$

$$\frac{\partial \bar{\psi}}{\partial Y}\frac{\partial \theta}{\partial X} + \frac{\partial \bar{\psi}}{\partial X}\frac{\partial \theta}{\partial Y} = \left(\frac{\partial^2 \theta}{\partial X^2} + \frac{\partial^2 \theta}{\partial Y^2}\right) \qquad (2.7)$$

With the non dimensionless boundary conditions are

U (X , 0) = U(X, 1) = U(0 , Y) = U(1 ,Y) = 0,

V (X , 0) = V(X, 1) = V(0 , Y) = V(1, Y) = 0,

θ (X, 0) =1, or θ (X, 0) = $\sin(\pi x)$, ,

$$\frac{\partial \theta}{\partial Y}(X, 1) = 0, \qquad \theta(0, Y) = \theta(1, Y) = 0$$

Here X and Y are dimensionless coordinates varying along horizontal and vertical directions; U and V are dimensionless velocity components along X and Y-directions; θ is the dimensionless temperature; P is the dimensionless pressure; Ra, Pr and Ar are Rayleigh number, Prandtl number and Aspect ratio respectively.

NUSSELT NUMBER (Nu)

The ratio of the conductive thermal resistance to the convective thermal resistance of the fluid is called Nusselt number. This is written as Nu = $\frac{hL}{K}$.

RAYLEIGH NUMBER (Ra)

The ratio of the apparent conductivity to the true molecular conductivity is a function, which is the product of Grashof number and prandtl number. This function is referred as the Rayleigh number.

i.e., Ra = $\frac{g\beta\Delta TL^3}{u\alpha}$.

GRASHOF NUMBER (Gr)

It plays a significant role in the natural convection heat transfer, the ratio of the product of the internal force and the buoyant force to the square of viscous force in the convective flow system is interpreted as Grashof number. In free convection, it is analogous to Reynolds number in forced convection.

PRANDTL NUMBER (Pr)

The ratio of the kinetic viscosity (ϑ) to the thermal diffusivity (α) of a fluid is called Prandtl number.

III. NUMERICAL SOLUTION

In the present study, we have predominantly used Galerkin Finite Element Method (FEM) except for one case in which Finite difference method was utilized, as it was particularly suitable for that case. The following sections enlighten the Finite element method and present its application to solve the above-mentioned equations.

FEM can be comprised roughly 5 steps to solve the particular problem. The steps are as follows.

- ✓ *DESCRITIZING THE DOMAIN:* This step involves the division of whole physical domain into smaller segments known as elements, and then identifying the nodes, coordinates of each node and ensuring proper connectivity between the nodes.
- ✓ *SPECIFYING THE EQUATION:* In this step, the governing equation is specified and an equation is written in terms of nodal values
- ✓ *DEVELOPMENT OF GLOBAL MATRIX:* The equations are arranged in a global matrix which takes into account the whole domain
- ✓ *SOLUTION:* The equations are solved to get the desired variable at each table in the domain
- ✓ *EVALUATE THE QUANTITIES OF INTEREST:* After solving the equations a set of values is obtained for each node, which can be further processed to get the quantities of interest.

There are varieties of elements available in FEM, which are distinguished by the presence of number of nodes. The present study is carried out by using a simple 3-noded triangular element.

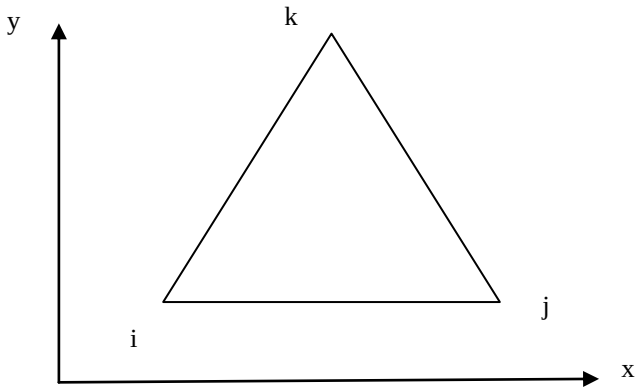

Typical triangular element

Let us consider that the variable to be determined in the triangular area is 'θ'. The polynomial function for 'θ' can be expressed as:

$$\theta = \alpha_1 + \alpha_2 x + \alpha_3 y$$

The variable θ has the value θ_i, θ_j and θ_k at the nodal position i, j and k of the element. The x and y coordinates at these points are x_i, x_j, x_k and y_i, y_j and y_k respectively. Substitution of these nodal values in θ, helps in determining the constants α_1, α_2, α_3 which are:

$$\alpha_1 = {}^1/_{2A}\left[(x_j y_k - x_k y_j)\,\theta_i + (x_k y_i - x_i y_k)\,\theta_j + (x_i y_j - x_j y_i)\,\theta_k\right]$$

$$\alpha_2 = {}^1/_{2A}\left[(y_j - y_k)\,\theta_i + (y_k - y_i)\,\theta_j + (y_i - y_j)\,\theta_k\right]$$

$$\alpha_3 = {}^1/_{2A}\left[(x_k - x_j)\,\theta_i + (x_i - x_k)\,\theta_j + (x_j - x_i)\,\theta_k\right]$$

where A is area of the triangle given as

$$2A = \begin{vmatrix} 1 & x_i & y_i \\ 1 & x_j & y_j \\ 1 & x_k & y_k \end{vmatrix}$$

Substitution of α_1, α_2, α_3 in θ and the mathematical arrangement of the terms results changed into

$$\theta = N_i\,\theta_i + N_j\,\theta_j + N_k\,\theta_k$$

Where N_i, N_j and N_k are the shape functions given by

$$N_m = \frac{a_m + b_m x + c_m y}{2A} \quad \text{for} \quad m = i, j, k$$

The constants can be expressed in terms of coordinates as

$a_i = x_j y_k - x_k y_j$	$b_i = y_j - y_k$	$c_i = x_k - x_j$
$a_j = x_k y_i - x_i y_k$	$b_j = y_k - y_i$	$c_j = x_i - x_k$
$a_k = x_i y_j - x_j y_i$	$b_k = y_i - y_j$	$c_k = x_j - x_i$

ISSN: 2394-4404

The triangular element can be subdivided into three triangles with a point in the center of original triangle.

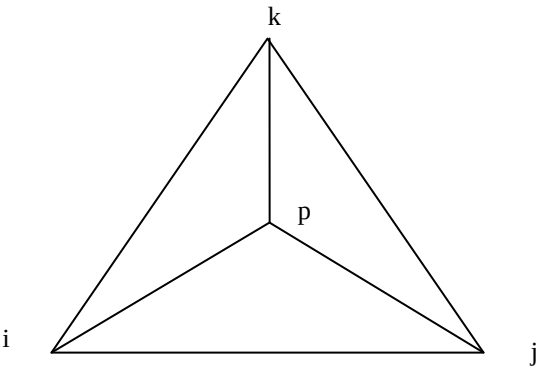

Sub triangular areas

Defining the new area ratios as

$$L_1 = \frac{area\ pij}{area\ ijk}; \quad L_2 = \frac{area\ pjk}{area\ ijk} \quad \text{and} \quad L_3 = \frac{area\ pki}{area\ ijk}$$

It can be shown that

$L_1 = N_1$; $L_2 = N_2$ and $L_3 = N_3$

Please note that the nodal terms *i, j & k* are replaced by 1, 2 & 3 respectively in subsequent discussions for simplicity.

The momentum and heat energy balanced equations are solved using the Galerkin finite element method. Continuity equation will be used as a constraint due to mass conservation and this constraint may be used to obtain the pressure distribution. In order to solve equations, we use the finite element method where the pressure P is eliminated by a penalty parameter γ and the incompressibility criteria given by equation (2.5) which results in

$$P = -\gamma\left(\frac{\partial \Psi}{\partial X} + \frac{\partial \theta}{\partial Y}\right)$$

The continuity equation (2.5) is automatically satisfied for large values of γ .

Application of Galerkin method to equation (2.6) yields:

$$\{R^e\} = -\int_A N^T \left\{\left[\frac{\partial \bar{\psi}}{\partial Y}\frac{\partial^2 \bar{\psi}}{\partial X \partial Y} - \frac{\partial \bar{\psi}}{\partial X}\frac{\partial^2 \bar{\psi}}{\partial Y^2}\right] - \Pr\left[\frac{\partial^2 \bar{\psi}}{\partial X^2} + \frac{\partial^2 \bar{\psi}}{\partial Y^2}\right] - \Pr\frac{\partial \bar{\psi}}{\partial Y} + Ra\Pr\theta\right\} dXdY \quad (2.8)$$

Where R^e is the residue.

Considering the terms individually

$$\int_A [N]^T \frac{\partial \bar{\psi}}{\partial Y}\frac{\partial^2 \bar{\psi}}{\partial X \partial Y} dA = \frac{1}{4A}\begin{Bmatrix} c_1\bar{\psi}_1 + c_2\bar{\psi}_2 + c_3\bar{\psi}_3 \\ c_1\bar{\psi}_1 + c_2\bar{\psi}_2 + c_3\bar{\psi}_3 \\ c_1\bar{\psi}_1 + c_2\bar{\psi}_2 + c_3\bar{\psi}_3 \end{Bmatrix} [b_1, b_2, b_3] \quad (2.9)$$

$$\int_A [N^T] \frac{\partial \bar{\psi}}{\partial X}\frac{\partial^2 \bar{\psi}}{\partial Y^2} dA = \frac{1}{12A}\begin{Bmatrix} b_1\bar{\psi}_1 + b_2\bar{\psi}_2 + b_3\bar{\psi}_3 \\ b_1\bar{\psi}_1 + b_2\bar{\psi}_2 + b_3\bar{\psi}_3 \\ b_1\bar{\psi}_1 + b_2\bar{\psi}_2 + b_3\bar{\psi}_3 \end{Bmatrix} [c_1, c_2, c_3] \quad (2.10)$$

$$\int_A [N^T] \Pr \frac{\partial^2 \bar{\psi}}{\partial X^2} dA = -\frac{\Pr}{4A}\begin{bmatrix} c_1^2 & c_1c_2 & c_1c_3 \\ c_1c_2 & c_2^2 & c_2c_3 \\ c_1c_3 & c_2c_3 & c_3^2 \end{bmatrix} \begin{bmatrix} \theta_1 \\ \theta_2 \\ \theta_3 \end{bmatrix} \quad (2.11)$$

$$\int_A [N^T] \Pr \frac{\partial^2 \bar{\psi}}{\partial Y^2} dA = -\frac{\Pr}{4A}\begin{bmatrix} b_1^2 & b_1b_2 & b_1b_3 \\ b_1b_2 & b_2^2 & b_2b_3 \\ b_1b_3 & b_2b_3 & b_3^2 \end{bmatrix} \begin{bmatrix} \theta_1 \\ \theta_2 \\ \theta_3 \end{bmatrix} \quad (2.12)$$

$$\text{But } \int_A [N]^T \Pr \frac{\partial \bar{\psi}}{\partial Y} dA = \Pr \int_A \begin{Bmatrix} L_1 \\ L_2 \\ L_3 \end{Bmatrix} \left(\left(\frac{\partial N}{\partial Y}\right)\{\bar{\psi}\}\right) dA$$

$$= \Pr \frac{1}{12A}\begin{bmatrix} 1 \\ 1 \\ 1 \end{bmatrix} \left[c_1\bar{\psi}_1 + c_2\bar{\psi}_2 + c_3\bar{\psi}_3\right] \quad (2.13)$$

$$\int_A [N]^T Ra \Pr \theta dA = \frac{Ra \Pr}{12A}\begin{bmatrix} \theta_1 \\ \theta_2 \\ \theta_3 \end{bmatrix} \quad (2.14)$$

Thus the whole equation (2.8) can be written in matrix form as

$$\frac{1}{4A}\begin{Bmatrix} c_1\bar{\psi}_1 + c_2\bar{\psi}_2 + c_3\bar{\psi}_3 \\ c_1\bar{\psi}_1 + c_2\bar{\psi}_2 + c_3\bar{\psi}_3 \\ c_1\bar{\psi}_1 + c_2\bar{\psi}_2 + c_3\bar{\psi}_3 \end{Bmatrix} [b_1, b_2, b_3] - \frac{1}{12A}\begin{Bmatrix} b_1\bar{\psi}_1 + b_2\bar{\psi}_2 + b_3\bar{\psi}_3 \\ b_1\bar{\psi}_1 + b_2\bar{\psi}_2 + b_3\bar{\psi}_3 \\ b_1\bar{\psi}_1 + b_2\bar{\psi}_2 + b_3\bar{\psi}_3 \end{Bmatrix} [c_1, c_2, c_3]$$

$$-\frac{\Pr}{4A}\begin{bmatrix} c_1^2 & c_1c_2 & c_1c_3 \\ c_1c_2 & c_2^2 & c_2c_3 \\ c_1c_3 & c_2c_3 & c_3^2 \end{bmatrix} \begin{bmatrix} \theta_1 \\ \theta_2 \\ \theta_3 \end{bmatrix} - \frac{\Pr}{4A}\begin{bmatrix} b_1^2 & b_1b_2 & b_1b_3 \\ b_1b_2 & b_2^2 & b_2b_3 \\ b_1b_3 & b_2b_3 & b_3^2 \end{bmatrix} \begin{bmatrix} \theta_1 \\ \theta_2 \\ \theta_3 \end{bmatrix}$$

$$-\Pr\frac{1}{12A}\begin{bmatrix} 1 \\ 1 \\ 1 \end{bmatrix} \left[c_1\bar{\psi}_1 + c_2\bar{\psi}_2 + c_3\bar{\psi}_3\right] + \frac{Ra \Pr}{12A}\begin{bmatrix} \theta_1 \\ \theta_2 \\ \theta_3 \end{bmatrix} = 0 \quad (2.15)$$

Application of Galerkin method to equation (2.7) yields:

$$\{R^e\} = -\int_A [N]^T \left(\frac{\partial \bar{\psi}}{\partial Y}\frac{\partial \theta}{\partial X} + \frac{\partial \bar{\psi}}{\partial X}\frac{\partial \theta}{\partial Y} - \frac{\partial^2 \theta}{\partial X^2} - \frac{\partial^2 \theta}{\partial Y^2}\right) dA \quad (2.16)$$

Now considering the terms individually

$$\int_A [N^T] \frac{\partial \bar{\psi}}{\partial X}\frac{\partial \theta}{\partial Y} dA = \frac{1}{12A}\begin{Bmatrix} b_1\bar{\psi}_1 + b_2\bar{\psi}_2 + b_3\bar{\psi}_3 \\ b_1\bar{\psi}_1 + b_2\bar{\psi}_2 + b_3\bar{\psi}_3 \\ b_1\bar{\psi}_1 + b_2\bar{\psi}_2 + b_3\bar{\psi}_3 \end{Bmatrix} [c_1, c_2, c_3] \begin{bmatrix} \theta_1 \\ \theta_2 \\ \theta_3 \end{bmatrix} \quad (2.17)$$

$$\int_A [N^T] \frac{\partial^2 \theta}{\partial X^2} dA = -\frac{1}{4A}\begin{bmatrix} b_1^2 & b_1b_2 & b_1b_3 \\ b_1b_2 & b_2^2 & b_2b_3 \\ b_1b_3 & b_2b_3 & b_3^2 \end{bmatrix} \begin{bmatrix} \theta_1 \\ \theta_2 \\ \theta_3 \end{bmatrix} \quad (2.18)$$

$$\int_A [N^T] \frac{\partial^2 \theta}{\partial Y^2} dA = -\frac{1}{4A}\begin{bmatrix} c_1^2 & c_1c_2 & c_1c_3 \\ c_1c_2 & c_2^2 & c_2c_3 \\ c_1c_3 & c_2c_3 & c_3^2 \end{bmatrix} \begin{bmatrix} \theta_1 \\ \theta_2 \\ \theta_3 \end{bmatrix} \quad (2.19)$$

Thus the whole equation (2.16) can be written in matrix form as

$$\frac{1}{12A}\begin{Bmatrix} c_1\bar{\psi}_1 + c_2\bar{\psi}_2 + c_3\bar{\psi}_3 \\ c_1\bar{\psi}_1 + c_2\bar{\psi}_2 + c_3\bar{\psi}_3 \\ c_1\bar{\psi}_1 + c_2\bar{\psi}_2 + c_3\bar{\psi}_3 \end{Bmatrix} [b_1, b_2, b_3] \begin{bmatrix} \theta_1 \\ \theta_2 \\ \theta_3 \end{bmatrix} - \frac{1}{12A}\begin{Bmatrix} b_1\bar{\psi}_1 + b_2\bar{\psi}_2 + b_3\bar{\psi}_3 \\ b_1\bar{\psi}_1 + b_2\bar{\psi}_2 + b_3\bar{\psi}_3 \\ b_1\bar{\psi}_1 + b_2\bar{\psi}_2 + b_3\bar{\psi}_3 \end{Bmatrix} [c_1, c_2, c_3] \begin{bmatrix} \theta_1 \\ \theta_2 \\ \theta_3 \end{bmatrix}$$

$$-\frac{1}{4A}\begin{bmatrix} b_1^2 & b_1b_2 & b_1b_3 \\ b_1b_2 & b_2^2 & b_2b_3 \\ b_1b_3 & b_2b_3 & b_3^2 \end{bmatrix} \begin{bmatrix} \theta_1 \\ \theta_2 \\ \theta_3 \end{bmatrix} + \frac{1}{4A}\begin{bmatrix} c_1^2 & c_1c_2 & c_1c_3 \\ c_1c_2 & c_2^2 & c_2c_3 \\ c_1c_3 & c_2c_3 & c_3^2 \end{bmatrix} \begin{bmatrix} \theta_1 \\ \theta_2 \\ \theta_3 \end{bmatrix} = 0 \quad (2.20)$$

IV. RESULTS AND DISCUSSIONS

Numerical results have been presented in order to determine the effects of presence of dimensionless parameters in a rectangular cavity. The dimensionless governing parameters which are specifically Nusselt numbers (Nu),

ISSN: 2394-4404

Aspect ratios (Ar), Rayleigh numbers (Ra), Prandtl number (Pr) and physical parameters length of the thin fin (L) and position of the fin on the cold wall(S).The presentation of the results have been started with streamlines and isotherms for various Rayleigh numbers and different position S= 0.25,0.5 and 0.75 and also for different Aspect ratios Ar= 4,2,1,0.5 and 0.25 having different fin lengths L= 0.5,0.75 and positions for fixed Pr = 1 is considered.

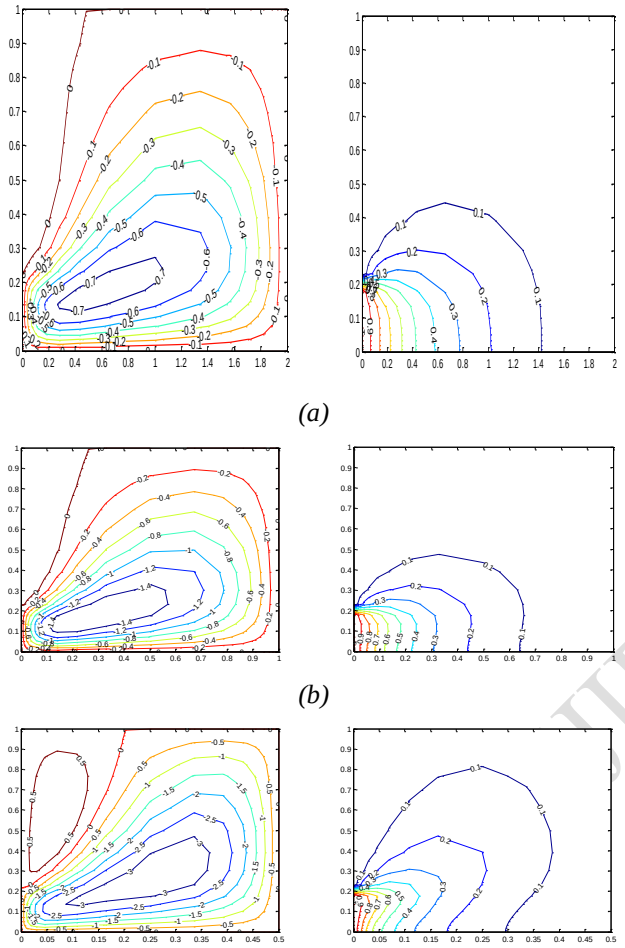

Figure 1: Contour plots for various Ra and different fin's S = 0.25. Clockwise and anti-clockwise flows are shown via negative and positive signs of stream functions (Left) and Isotherms (Right) respectively

Figs. 1 shows the streamlines and the isotherms for a square cavity with a fin at its lower position (S = 0.25), and for various *Ra* and different lengths of the fin, L = 0.25, 0.5 and 0.75, respectively.

For the all values of *Ra*, a large clockwise (CW) rotating cell is observed for all fin lengths. The fluid that is heated next to the hot wall (left wall) rises and replaces the cooled fluid next to the cold wall (right wall) that is falling, thus giving rise to a CW rotating vortex (also called the primary vortex).

Due to this figure, as the Rayleigh number increases, the flow patterns and the temperature distribution change from the conduction to convection dominated regime for all the L values. It seems that the various lengths of the fin not only change the flow fields near the fin, but they also relatively change the strength of the CW vortex. This is because the fin blocks the movement of the fluid and weakens the CW vortex. The flow and the temperature fields in the cavity, due to the streamlines and the isotherms, are presented.

In Fig. 2 for the middle position of a fin (S =0.5), and Fig. 3 for a fin at its upper position (S = 0.25) have been discussed.

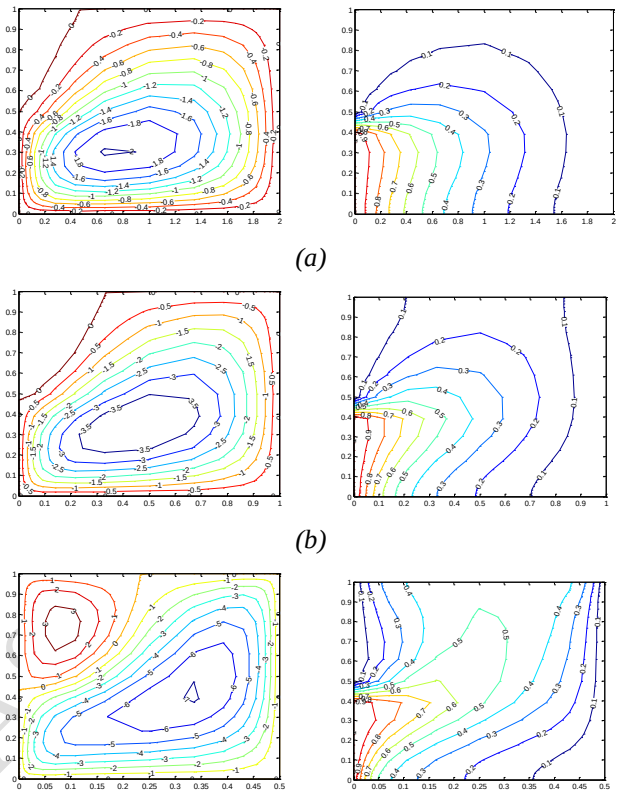

Figure 2: Contour plots for various Ra and different fin's S = 0.5. Clockwise and anti-clockwise flows are shown via negative and positive signs of stream functions (Left) and Isotherms (Right) respectively

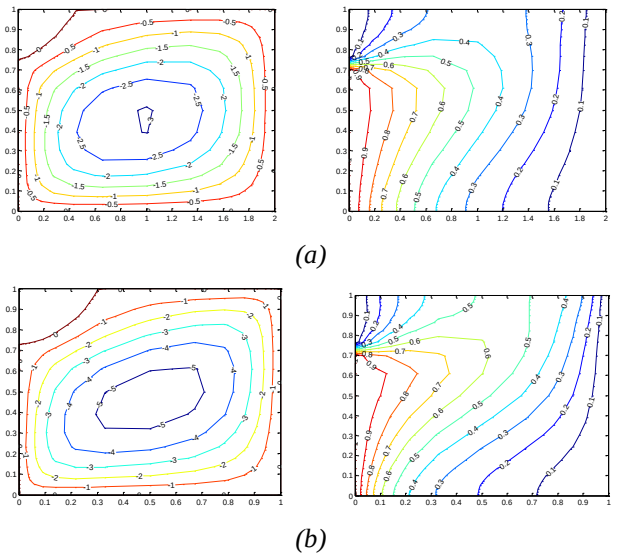

ISSN: 2394-4404

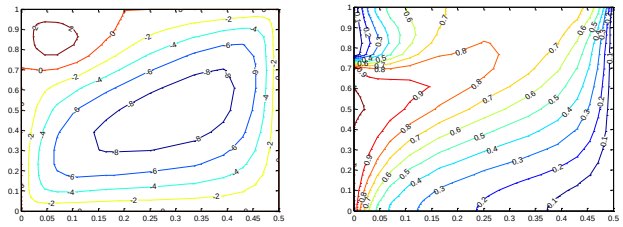

Figure 3: Contour plots for various Ra and different fin's S = 0.75. Clockwise and anti-clockwise flows are shown via negative and positive signs of stream functions (Left) and Isotherms (Right) respectively

By increasing the Rayleigh number, similar treatment corresponding to the flow and temperature distribution can be seen between these figures and those of Fig. 1, respectively.

By comparing all the cases in Figs. 1,2,3, it is possible to see that a fin attached to the middle of the wall has the most remarkable effect on the fluid flow in the cavity. A fin redirects the movement of the fluid and weakens the fluid motion within the area under the fin for $S < 0.5$, whereas it weakens the fluid motion within the area above the fin while $S \leq 0.5$.

V. EFFECT OF RAYLEIGH NUMBER

For $Ra = 10^4$, the streamlines and the isotherms near the fin exhibit similar trends as those for $Ra = 10^3$, and in some instances, the flow field exhibits two local minima that may be reminded for the common cases of a cavity with no fin. At the moderate Rayleigh numbers ($Ra = 10^5$), the boundary layer regime is developed towards the cavity walls and for higher *Ra*, the convective mode of heat transfer is dominated throughout the cavity. Moreover, the more packed stream function Rayleigh number increases. For the case of $Ra = 10^4$ (convection not being strong compared to conduction), presence of the fin brings resistance to the motion of the CW vortex and it has the most remarkable effects on the flow field when it is placed at the middle of the left wall.

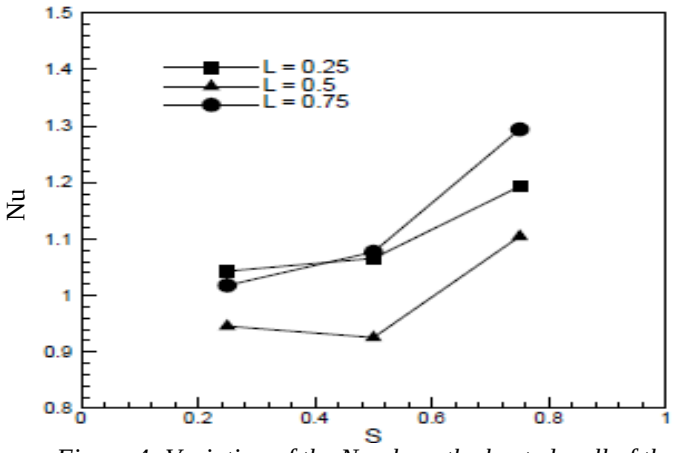

Figure 4: Variation of the Nu along the heated wall of the cavity with respect to position of the fin with Ra= 10^4

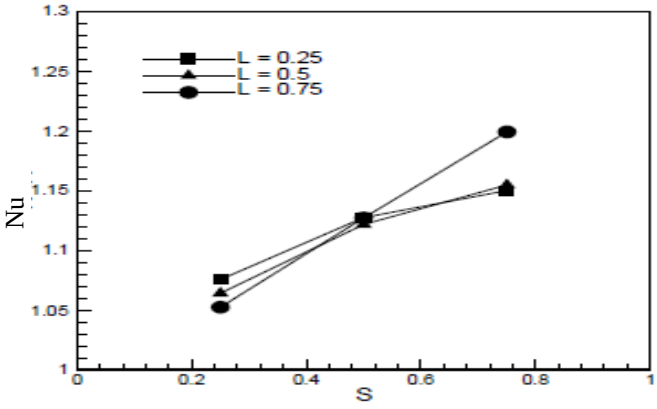

Figure 5: Variation of the Nu along the heated wall of the cavity with respect to position of the fin with Ra= 10^5.

It is observed that for the case of $Ra = 10^5$ (convection dominating conduction), a fin can block the flow, thus weakening the primary vortex, but at the same time a long enough cold fin can cools the fluid and make it lighter resulting in enhancement of the CW vortex. These two mechanisms are found to certainly counter balance each other for nearly the fin's middle position, regardless of the fin's length.

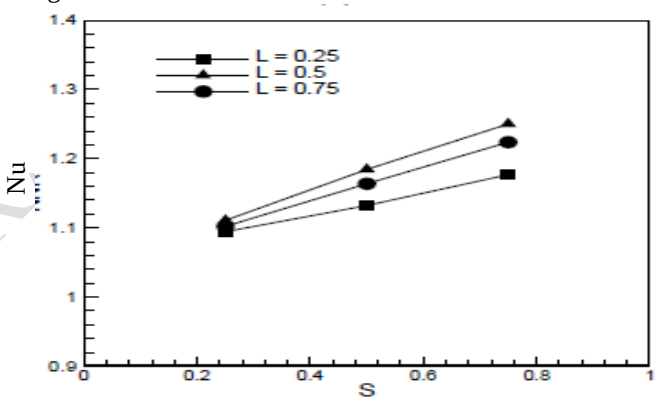

Figure 6: Variation of the Nu along the heated wall of the cavity with respect to position of the fin with Ra= 10^6

At $Ra = 10^6$, given the strong effect of free convection implies that placing a fin of any length can always enhance the primary vortex regardless of its position. It should be noted that at $Ra = 10^6$ the fin's effect of blocking the fluid motion is more dominant than effect of cooling the fluid to enhance the primary vortex.

Figures 4, 5 and 6 shows the variations of *NNR* with respect to the fin's position for three different lengths of the fin, $L = 0.25$, 0.5, and 0.75 for $Ra = 10^4$ to 10^6, respectively. Based on these figures, it is observed that placing a fin on the right wall always increases the heat transfer in cavity, except that for $Ra = 10^4$, when $L = 0.5$, and $0.25 \leq S \leq 0.5$. For $Ra = 10^4$, the effect of the fin's length on the mean heat transfer is more remarkable for longer fin's lengths, regardless of the fin's position, *S*. See that the effect of the fin's length on *NNR* becomes less remarkable with the rise of the Rayleigh number due to the fact that these three curves come closer. This is because the effect of the cold fin cooling the flow and enhancing the primary vortex can compensate the effect of the fin blocking the flow.

ISSN: 2394-4404

VI. EFFECT OF TEMPERATURE FIELDS

The value of θ on the left wall is 1. Comparing these figures for $Ra = 10^6$, a fin with $L = 0.25$ at most positions only changes the temperature distribution locally and the rest of the cavity remains unaffected. This is because the CW vortex has not altered too much upon introduction of a 0.2 W long fin and the fin only changes the velocity distribution locally. As mentioned before, a fin at $S < 0.5$ can weaken the fluid motion in the area below the fin and thus decreased heat transfer capability is expected.

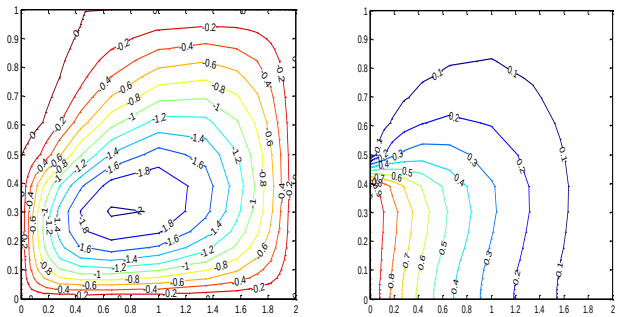

(a)

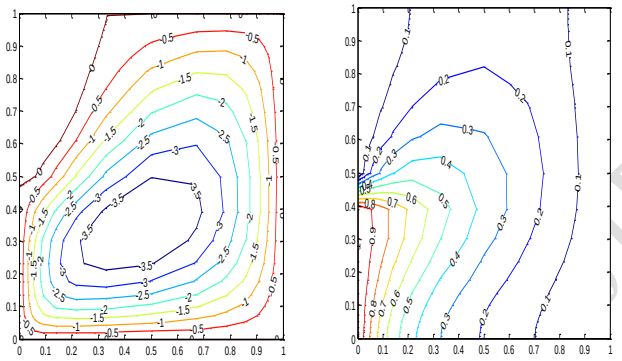

(b)

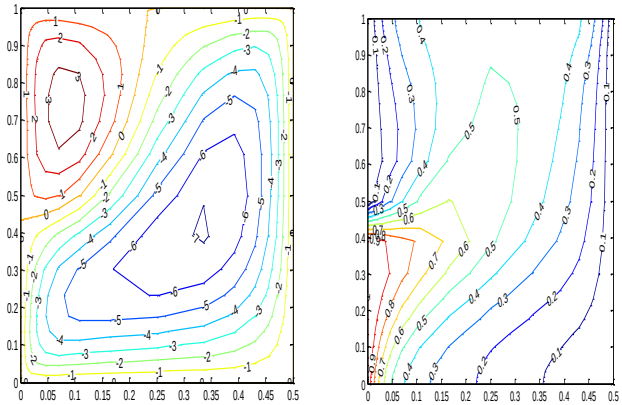

(c)

Figure 7: Contour plots for inside the rectangular cavity with Ar = 4 having a fin with L = 0.5 and S = 0.75 for Pr = 1 and various Ra. Clockwise and anti-clockwise flows are shown via negative and positive signs of stream functions (Left) and Isotherms (Right) respectively

Streamlines and isotherms for the cavity with $Ar = 4$ for different Rayleigh numbers are shown in Fig. 7. It is evident from the figure that for all Rayleigh numbers considered, two eddies are developed inside the enclosure which with an increase in Rayleigh number, the eddy located over the fin becomes weaker than that located under the fin. From the isotherms, a conduction dominant heat transfer is observed at $Ra = 10^4$ and 10^5.

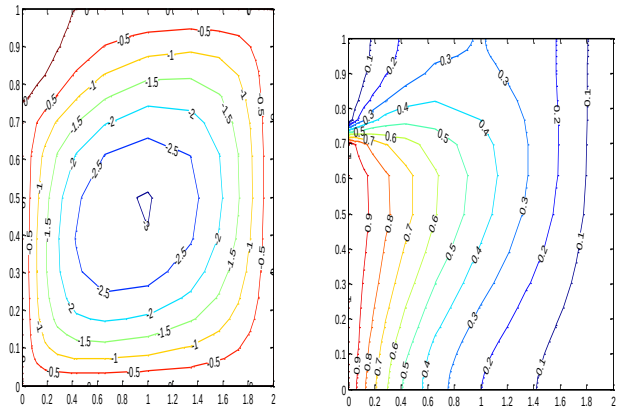

(a)

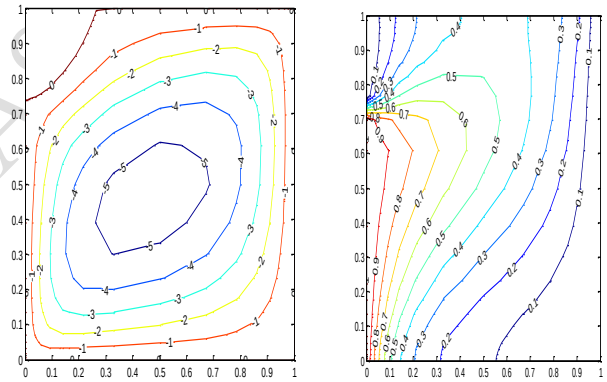

(b)

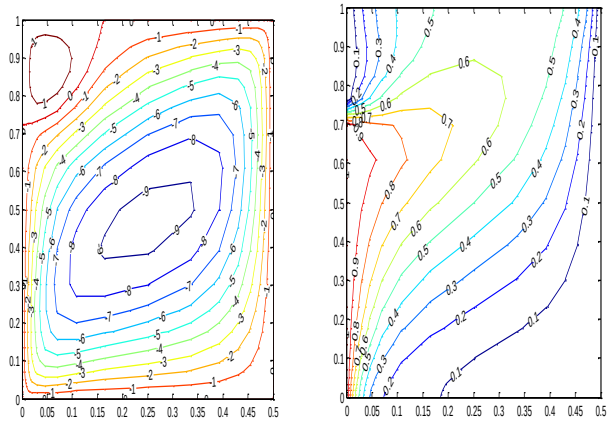

Figure 8: Contour plots for inside the rectangular cavity with Ar = 2 having a fin with L = 0.75 and S = 0.75 for Pr = 1 and various Ra. Clockwise and anti-clockwise flows are shown via negative and positive signs of stream functions (Left) and Isotherms (Right) respectively

ISSN: 2394-4404

At $Ra = 10^6$ thermal boundary layers are formed adjacent to the vertical walls and thermal stratification occurs in the region over the fin Variations of streamlines and isotherms inside the cavity with $Ar = 2$ versus Rayleigh number are shown in Fig. 8. It is observed that at $Ra = 10^4$ a clockwise eddy is formed under the fin and the fluid existing over the fin, is relatively stagnant. By increasing the buoyancy force at $Ra = 10^5$, a weak eddy is developed over the fin. Further increase in buoyancy force at $Ra = 10^6$ the strength of the eddy under the fin increases and it penetrates over the fin. Based on the isotherms it is evident that at $Ra = 10^4$ the heat transfer occurs mainly through conduction while with further increase in the Rayleigh number, the isotherms become more condensed adjacent to the vertical walls which is the characteristics of the natural convection.

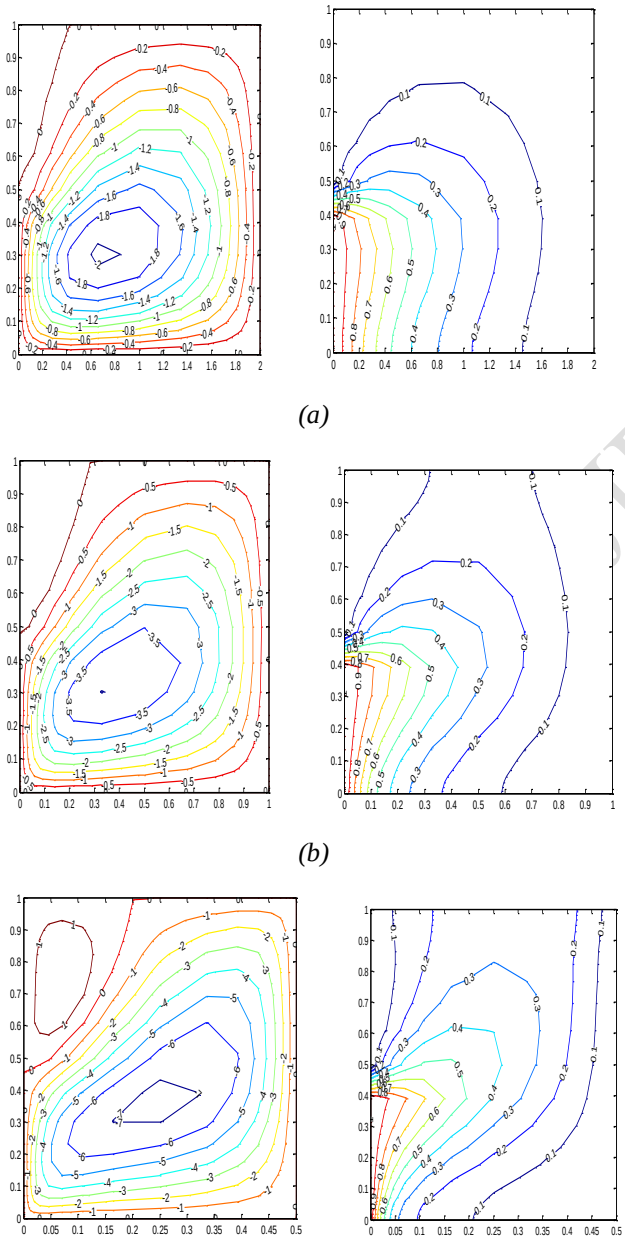

Figure 9: Contour plots for inside the rectangular cavity with Ar = 1 having a fin with L = 0.5 & S = 0.75 for Pr = 1 and various Ra. Clockwise and anti-clockwise flows are shown via negative and positive signs of stream functions (Left) and Isotherms (Right) respectively.

Fig. 9 shows streamlines and isotherms inside the cavity with $Ar = 1$ at different Rayleigh numbers. Similar to the results of the cavity with $Ar = 2$, at $Ra = 10^4$ the fluid over the fin is relatively stagnant and there is only an eddy under the fin. By increasing Rayleigh number, this eddy becomes stronger and penetrates over the fin. The mentioned observations about the isotherms of the cavity with $Ar = 2$ are valid here.

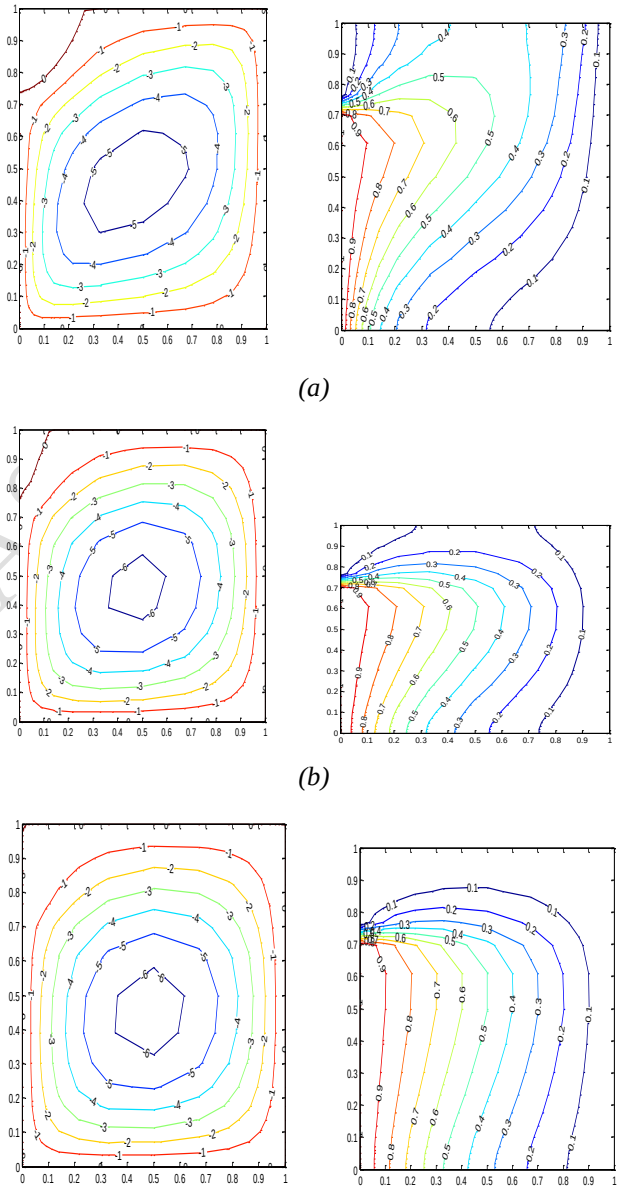

Figure 10: Contour plots for inside the rectangular cavity with Ar = 0.5 having a fin with L = 0.75 and S = 0.75 for Pr = 1 and various Ra. Clockwise and anti-clockwise flows are shown via negative and positive signs of stream functions (Left) and Isotherms (Right) respectively

ISSN: 2394-4404

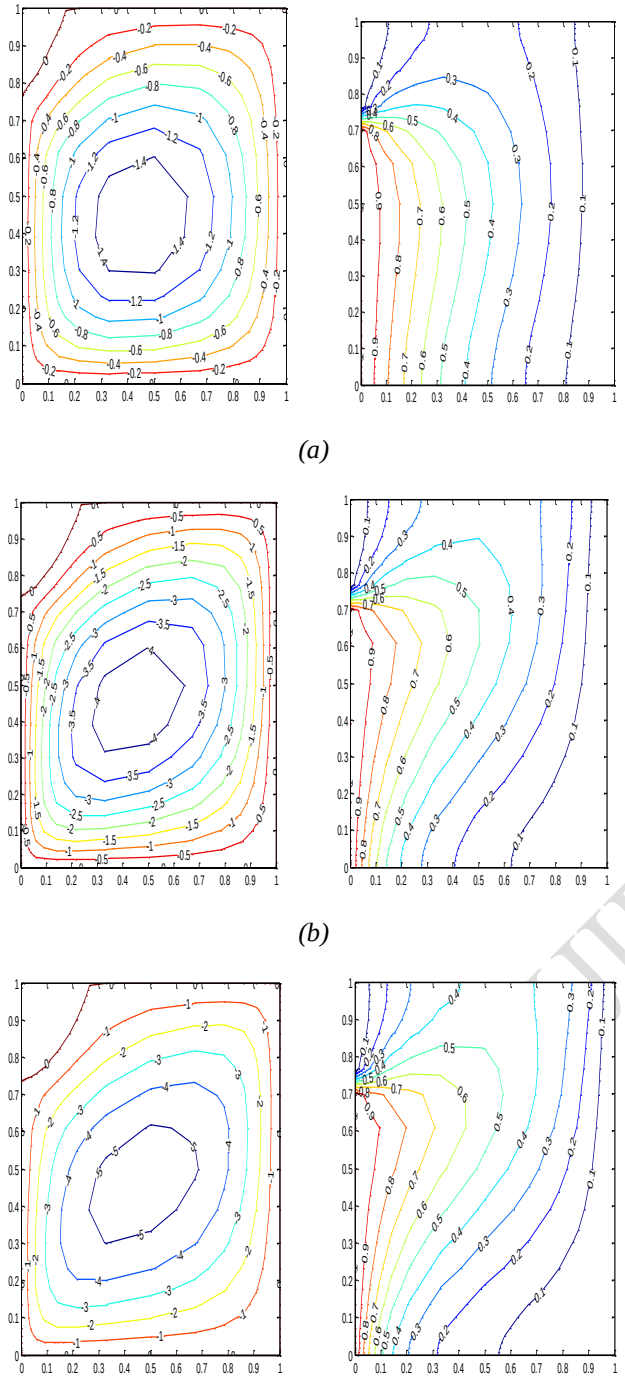

Figure 11: Contour plots for inside the rectangular cavity with Ar = 0.25 having a fin with L = 0.75 and S = 0.75 for Pr = 1 and various Ra. Clockwise and anti-clockwise flows are shown via negative and positive signs of stream functions (Left) and Isotherms (Right) respectively

The streamlines and isotherms inside the cavities with *Ar* = 0.5 and 0.25, at different Rayleigh numbers are shown in Figs. 10 and 11, respectively. As can be seen from the figures for two cavities with different aspect ratios, at $Ra = 10^4$ a clock wise eddy is developed under the fin. By increasing Rayleigh number the eddy penetrates over the fin and its central region is elongated horizontally. Conduction dominant heat transfer at $Ra = 10^4$ and formation of thermal boundary layers adjacent to the vertical walls at high Rayleigh numbers, is observed.

VII. EFFECT OF AVERAGE HEAT TRANSFER

In order to study the effect of the fin on the average heat transfer rate in the cavity, a variable named *NNR* is used which can be obtained. Value of *NNR* greater than 1 indicates that the heat transfer rate is enhanced in the cavity, whereas reduction of heat transfer is indicated when *NNR* is less than 1.

VIII. EFFECT OF NUSSELT NUMBER ON PRANDTL NUMBER AND ASPECT RATIOS

Variations of *NNR* with respect to Rayleigh number for different Prandtl numbers are shown in Fig. 12. According to the figure, as the cavity becomes narrower, the effect of fin on enhancement of heat transfer increases.

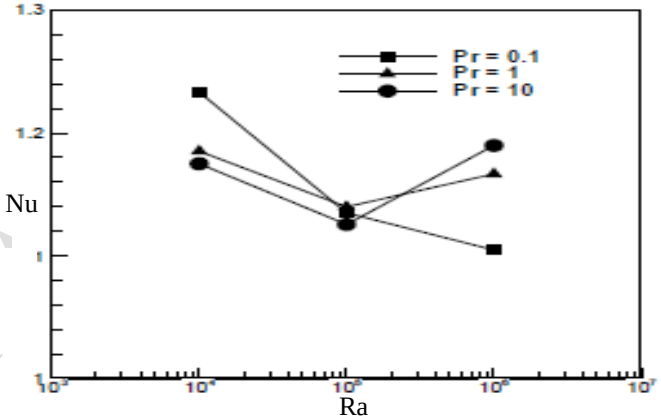

Figure 12: Variation of Nu along the heated wall of the cavity having a fin with L = 0.75 and S = 0.5 versus Pr.

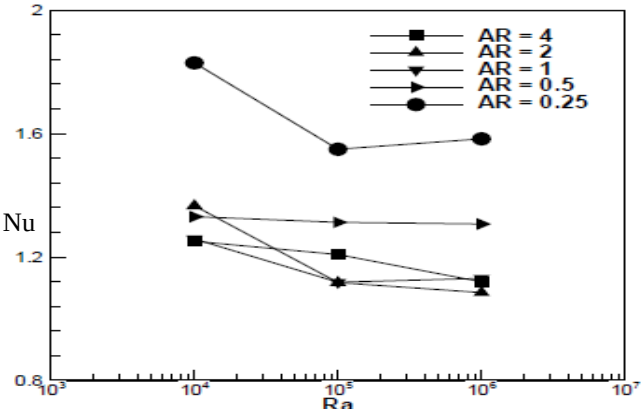

Figure 13: Variation of Nu along the heated wall of the cavity having a fin with L= 0.75 and S = 0.75 versus Ar

IX. CONCLUSIONS

- ✓ For the all values of *Ra*, a large clockwise (CW) rotating cell is observed for all fin lengths.
- ✓ The Rayleigh number increases, the flow patterns and the temperature distribution change from the conduction to convection dominated regime for all the *L* values. It

seems that the various lengths of the fin not only change the flow fields near the fin.

- ✓ The presence and the character of the primary CW rotating vortex is unaltered, with longer fin bringing about more changes to the flow compared to a shorter fin.
- ✓ The strong effect of free convection implies that placing a fin of any length can always enhance the primary vortex regardless of its position.
- ✓ At the higher Rayleigh numbers, the temperature contours above the fin are more packed than those under the fin. This implies better heat transfer on the top surface of the fin than on the bottom surface for almost all mentioned values of S.
- ✓ For longer fins, the temperature contours to the left of the fin are affected by the introduction of the fin.
- ✓ The average Nusselt number can be obtained from the product of *NNR* and average Nusselt number for a no-fin cavity
- ✓ The heat transfer occurs mainly through conduction while with further increase in the Rayleigh number, the isotherms become more condensed adjacent to the vertical walls which is the characteristics of the natural convection.
- ✓ Variations of *NNR* with respect to Rayleigh number for different Prandtl numbers, as the cavity becomes narrower, the effect of fin on enhancement of heat transfer increases.

REFERENCES

[1] Frederick, R. L., "Natural Convection in an Inclined Square Enclosure with a Partition Attached to Its Cold Wall", International Journal of Heat and Mass Transfer, Vol. 32, pp. 87–94, 1989.

[2] Frederick, R. L., Valencia, A., "Heat Transfer in a Square Cavity with a Conducting Partition on Its Hot Wall", International Communication of Heat and Mass Transfer, Vol. 16, pp. 347–354, 1989.

[3] Scozia, R., Frederick, R.L., "Natural Convection in Slender Cavities with Multiple Fins Attached on an Active Wall", Numerical Heat Transfer, Part A, Vol. 20, pp. 127–158, 1991.

[4] Nag, A., Sarkar, A., Sastri, V.M.K., "Natural Convection in a Differentially Heated Square Cavity with a Horizontal Partition Plate on the Hot Wall", Computer

[5] Methods in Applied Mechanics and Engineering, Vol. 110, pp. 143–156, 1993.

[6] Lakhal, E. K., Hasnaousi, M., Bilgen, E., Vasseur, P., "Natural Convection in Inclined Rectangular Enclosures with Perfectly Conducting Fins Attached on the Heated Wall", Heat and Mass Transfer, Vol. 32, pp. 365–373, 1997.

[7] Bilgen, E., "Natural Convection in Enclosures with Partial Partitions", Renewable Energy, Vol. 26, pp. 257–270, 2002.

[8] Shi, X., Khodadadi, J.M., "Laminar Natural Convection Heat Transfer in a Differentially Heated Square Cavity Due to a Thin Fin on the Hot Wall", ASME Journal of Heat Transfer, Vol. 125, pp. 624–634, 2003.

[9] S.H.Tasnim, M.R.Collins, "Numerical analysis of heat transfer in a square cavity with a baffle on the hot wall", Int. Commutative heat mass transfer, 31 (2004), PP.639-650.

[10] E.Bilgen, "Natural convection in cavities with a thin fin on the hot wall", Int. J. Heat mass transfer, 48(2005), PP .3493-3505.

[11] F.Xu, J.C.Patterson, C.Lei, "The effect of the thin fin length on the transition of the natural convection flows in a differentially heated cavity", Int.J. Therm.Sci, 70(2013), PP.92-101.

[12] Y. Liu, C.Lei, J. C. Patterson, "Natual convection in a differentially heated cavity with two horizontal adiabatic fins on the side walls. Int. J.Heat mass transfer, 72 (2014), PP. 23-36.